Interallelic Complementation at the *Drosophila melanogaster gastrulation defective* Locus Defines Discrete Functional Domains of the Protein

Gregory Ponomareff,* Heidi Giordano,† Yvonne DeLotto‡ and Robert DeLotto‡

**Cornell Graduate School of Medicine, New York, New York 10021,* ‡*Department of Genetics, University of Copenhagen, Copenhagen K, Denmark and* †*Tularik, South San Francisco, California 94080*

Manuscript received February 28, 2001
Accepted for publication July 11, 2001

ABSTRACT

The *gastrulation defective* (*gd*) locus encodes a novel serine protease that is involved in specifying the dorsal-ventral axis during embryonic development. Mutant alleles of *gd* have been classified into three complementation groups, two of which exhibit strong interallelic (intragenic) complementation. To understand the molecular basis of this interallelic complementation, we examined the complementation behavior of additional mutant alleles and sequenced alleles in all complementation groups. The data suggest that there are two discrete functional domains of Gd. A two-domain model of Gd suggesting that it is structurally similar to mammalian complement factors C2 and B has been previously proposed. To test this model we performed SP6 RNA microinjection to assay for activities associated with various domains of Gd. The microinjection data are consistent with the complement factor C2/B-like model. Site-directed mutagenesis suggests that Gd functions as a serine protease. An allele-specific interaction between an autoactivating form of Snake (Snk) and a *gd* allele altered in the protease domain suggests that Gd directly activates Snk in a protease activation cascade. We propose a model in which Gd is expressed during late oogenesis and bound within the perivitelline space but only becomes catalytically active during embryogenesis.

DORSAL-VENTRAL polarity of the Drosophila embryo is established during embryogenesis by the interpretation of positional information that is placed in the egg during oogenesis. Consequently, the process of specifying dorsal-ventral cell fate can be viewed as occurring in two distinct phases: an early one of producing a stable asymmetric cue in the mature egg and a later one involving interpretation of that positional cue at the syncytial blastoderm stage. Both phases of this process rely extensively upon signal transduction mechanisms (Stein *et al.* 1991; Roth *et al.* 1995). The establishment of polarity in the egg involves reciprocal signaling between the somatic follicle cells and the germ-line-derived ooplasm and requires the products of the genes *gurken*, a TGF-α homolog, and *torpedo*, the Drosophila epidermal growth factor receptor (Schüpbach 1987; Clifford and Schüpbach 1992; Neuman-Silberberg and Schüpbach 1993). Signaling during oogenesis serves to suppress ventral cell fate on the dorsal side of the developing oocyte. Further downstream in the pathway, the products of the genes *nudel*, *windbeutal*, and *pipe* are required to create a highly stable asymmetric cue that polarizes subsequent patterning during embryo-genesis (reviewed by Morisato and Anderson 1995).

The second phase, that of interpretation of the cue during embryogenesis, involves another signal transduction pathway in which a signal originates within the perivitelline space (PVS) of the embryo (Stein *et al.* 1991). There, a ventrally restricted extracellular signal results in the activation of the plasma membrane receptor Toll on the ventral side of the syncytial blastoderm embryo. This asymmetric activation of Toll directs the formation of a gradient of the transcription factor, Dorsal, along the dorsal-ventral axis of the cellular blastoderm embryo (Steward *et al.* 1988; Roth *et al.* 1989; Rushlow *et al.* 1989). As a result, blastoderm nuclei in ventral positions acquire higher concentrations of Dorsal protein while nuclei at more dorsal positions acquire lower concentrations. As a function of their nuclear Dorsal concentrations, blastoderm cells will differentiate with correct dorsal-ventral cell fates according to their relative position.

An outstanding question is how the positional information laid down in the egg is converted into the ventrally restricted signal within the PVS after fertilization (reviewed by Roth 1994). Part of the mechanism appears to involve a proteolytic activation cascade (DeLotto and Spierer 1986; Chasen and Anderson 1989). Several serine proteases sequentially activate each other in a proteolytic activation cascade and ultimately process Spaetzle (Spz), a precursor of an NGF-like growth factor ligand (Morisato and Anderson 1994; DeLotto and DeLotto 1998; Dissing *et al.* 2001; LeMosy *et al.* 2001). Epistasis data from microinjection experiments place

Corresponding author: Robert DeLotto, Department of Genetics, University of Copenhagen, Copenhagen K, Denmark.
E-mail: rdelotto@biobase.dk

another gene product, that of the *gd* gene, upstream of *snake* (*snk*) in the pathway (Smith and DeLotto 1994).

The molecular cloning of *gd* showed it to encode a protein with homology to the serine proteinase superfamily with, however, several structural features that are unusual for members of that superfamily (Konrad *et al.* 1998). A structural model for Gd, which is consistent with it being a functional serine protease with a structure analogous to the mammalian complement factors C2 and B, has been proposed (DeLotto 2001). Recent biochemical studies indicate proteolytic activity for Gd (Dissing *et al.* 2001; LeMosy *et al.* 2001). Microinjection of *in vitro*-synthesized *gd* wild-type mRNA was shown to rescue the dorsalized phenotype of embryos derived from *gd* null homozygous females. Furthermore, the dosage of Gd had a primary effect upon the magnitude of the ventralizing signal (DeLotto 2001).

gd, a genetically complex locus at cytological location 11A, was first described in a genetic screen for maternal effect genes affecting embryonic development (Mohler 1977). Twelve mutant alleles were later characterized in an extensive genetic analysis and the data clearly indicated complex interallelic complementation (Konrad *et al.* 1988a,b). While all mutant alleles were fully recessive and allelic to *gd* by virtue of their failure to complement some alleles of *gd*, genetic complexity was evident in certain heterozygous combinations. For example, both gd^2/gd^2 females and gd^{10}/gd^{10} females produced completely dorsalized eggs and are amorphic by virtue of no change in phenotypic strength when either gd^2 or gd^{10} is placed over *Df(1)KA10*, a deficiency overlapping *gd*. However, gd^2/gd^{10} females produced phenotypically normal first instar larvae, some of which developed to adults. Clonal analysis revealed that *gd* function is required in the germ line and the analysis of temperature-sensitive (ts) alleles revealed a broad ts period, which includes the last 4–5 hr of oogenesis and extends into the first 1.5–2 hr of embryogenesis. This contrasts with *ea*, which during embryogenesis has a ts period between 0 and 3 hr after fertilization (Anderson and Nüsslein-Volhard 1984, 1986). This would suggest that while Gd is needed both during late oogenesis and into early embryogenesis, Ea appears to be required only during embryogenesis. This temporal difference in the requirements of *gd* and *ea* is puzzling in light of the biochemical demonstration that Gd and Ea function via Snk in a sequential proteolytic cascade during embryogenesis (Dissing *et al.* 2001).

The structural model for Gd suggests that it is similar to the mammalian complement factors C2 and B, two unusual serine proteases involved in the classical and alternative pathways of activation of the complement cascade (DeLotto 2001). Almost all serine proteases are activated by cleavage at a region called the activation peptide, usually resulting in an isoleucine or valine at the amino terminus of the active catalytic chain (reviewed by Stroud *et al.* 1977). Indeed, Snk and Ea have such a stereotypical structure (DeLotto and Spierer 1986; Chasen and Anderson 1989). Gd lacks significant homology to the serine protease superfamily in the activation peptide region (Konrad *et al.* 1998). However, it does have an arginine lysine pair followed by homology to a vonWillebrand factor type A (vWF) motif within the polypeptide chain. The vWF domain constitutes a binding site for an activating protease in complement factors C2 and B (Oglesby *et al.* 1988). In complement factors C2 and B, activation results in a cleavage between the arginine and lysine residues to generate two distinct polypeptide chains (reviewed by Arlaud *et al.* 1998).

To understand the basis of the interallelic complementation at *gd*, we extended the complementation analysis to more recently isolated *gd* alleles and determined the molecular lesions associated with alleles in all complementation groups. To test the C2/B structural model of Gd, we used an SP6 RNA microinjection assay to assay for activities of discrete domains of Gd. Our data support processing of Gd in a manner consistent with the complement C2/B-like model. An allele-specific interaction using RNA microinjection is consistent with biochemical data indicating that Gd directly activates Snk in a proteolytic cascade. Finally, we propose a biological model in which an inactive form of Gd is bound to a membrane within the PVS late during oogenesis but only becomes activated later at syncytial blastoderm stage. Such a model can account for the earlier-starting ts period described for *gd* as well as accommodate a direct role of Gd in activating the Snk zymogen in the protease cascade.

MATERIALS AND METHODS

Fly strains used: Wild-type strains were Oregon-R. The genotypes and sources of the alleles are as follows. gd^1 v^{24}*/FM3*, gd^2 *v/FM3*, gd^3 *v/FM3*, gd^4 *v/FM3*, gd^5 *v/FM3*, gd^6 *v/FM3*, gd^7 *v/FM3*, and gd^{190}*/FM7*, *l(1) TW9* were from the Tübingen stock collection. gd^{m27} *y/FM7*, gd^{p18} *y/FM7*, gd^9 *v/FM3*, and gd^{10} *v/FM3* were provided by K. Konrad. *gd* alleles prefixed by V, T, and L, marked with *y w P[w+FRT]*, and balanced over *FM7c* were isolated and kindly provided by T. Schüpbach. *Df(1)KA10* sn^3 *m/FM7c* was from the Bloomington stock collection.

Cuticle preparations and complementation analysis: The collection of embryos, dechorionation of embryos, and preparation of cuticles were performed as described (Wieschaus and Nüsslein-Volhard 1986). Slides of prepared cuticles were examined under darkfield or phase microscopy.

***rhomboid in situ* hybridization of Drosophila embryos:** *In situ* hybridizations were performed as described (Roth 1994; Roth and Schüpbach 1994). *rho* cDNA was a generous gift from E. Bier, and the probe was made according to the Boehringer-Mannheim (Roche, Indianapolis) protocol using the SP6/T7 DIG RNA labeling kit. After staining, embryos were cleared and mounted with Permount (Fisher, Pittsburgh).

Cloning of the *gd* mutant alleles: Genomic DNA was prepared as follows: 50–100 males of the appropriate stock were homogenized in TE and phenol (pH 8) 1:1. Nucleic acids were isopropanol precipitated, dried, and resuspended in 50–100 ml of TE. DNA (0.5 ml) was added to a 25-ml PCR reaction with the 5′ *gd* genomic and 3′ *gd* genomic flanking primers

TABLE 1

Oligonucleotide primers used in cloning, sequencing, and injection constructs

Name of primer	Restriction sites	*gd* cDNA sequence	Oligonucleotide sequence (5′–3′)
5′ *gd* genomic	*Xba*I, *Bgl*II	−34 to 16	agtcgtctagagatctattttcatcccgggcatt
3′ *gd* genomic	*Eco*RI, *Kpn*I	15–33 past STOP	agtccgaattcggtaccgcgttcccatacacattt
5′ *gd* coding	*Sal*I, *Bgl*II	1–21	aggtcgacagatctatgaggctgcacctggcggcg
3′ *gd* coding	*Pst*I, *Kpn*I	1584–1563	agctgcagggtaccaattacaaaggccgtgatcca
gd seq.1	—	179–196	gagttacgctctcgatgc
gd seq.2	—	379–397	atgacccaaatccagttg
gd seq.3	—	584–602	acttgtcccaaagaacgg
gd seq.4	—	781–799	tggctagcggccatctat
gd seq.5	—	981–999	cgtcgatggcatttacat
gd seq.6	—	1181–1199	acaggacgcgggatcaga
gd seq.7	—	1360–1377	cgagatacgcatcagagc
gd seq.1.5	—	232–249	gagctactcacacgcggc
5′ *tsg*	*Eco*RI	*tsg* 1266–1283	agtcggaattcagcttggacctcatcata
gd 1244–1229(3′)	—	1244–1229	gcactggcatcggtgg
118.12	—	251–235	ttcgccgcgtgtgagtag
120.3	—	427–411	ccggtataaaggacaact
121.10	—	633–616	ctttggttcaccgattgc
121.12	—	786–769	tagccaaggccacgatcc
118.9	—	Intron 4-1083	acgcagtttaacacc
gd 3′ pro-enz	*Not*I	410–390	agtcgtcaggcggccgctactacctaatgtgctccaactgg
3′ *gd* vWF e	*Eco*RI	749–736	gcacggaattctactagctatcggcgctatc
5′ *easter-gd* cat	Fusion	*ea* sig-*gd* cat	gcgaaatcatcggcgggcaagttgtcctttataccg
3′ *gd* cat-*ea* sig pep	Fusion	*gd* cat-*ea* sig	cggtataaaggacaacttgcccgccgatgatttcgc
easter 5′	*Bgl*II	*easter* 1–15	gctgaagatctatgctaaagccatcg

listed in Table 1. After PCR, the fragments were digested with *Eco*RI and *Bgl*II restriction enzymes, gel purified, and cloned into pGEM3. For the generation of cDNA clones from wild type and the *gd* mutant alleles, 0- to 2-hr embryos or homozygous females were homogenized in a Dounce with 0.5 ml of 4 M guanidinium isothiocyanate, 5 mM dithiothreitol, and 0.4 ml acid phenol. After two acid phenol/chloroform extractions and one chloroform extraction, nucleic acids were precipitated and poly(A)$^+$ RNA was purified as described in Sambrook (1989). RNA (3 mg) was used in an RT-PCR reaction (as described in DeLotto *et al.* 2001) using the 5′ *gd* genomic and 3′ *gd* genomic flanking primers listed in Table 1. The PCR product was digested with *Eco*RI and *Bgl*II and ligated directionally into SP64-T. DNA sequencing reactions were performed on double stranded plasmid DNA using Sequenase Version 2 (USB) according to the manufacturer's protocols using primers listed in Table 1.

***gd* domain constructs:** gdΔn_e was made by fusing the signal peptide sequence of Ea to the vWF and serine protease domains of *gd* as described in Higuchi (1990). The outside primers were 5′ easter *Bgl*II and 3′ *gd* genomic. The inside primers were 5′ easter-gd cat and 3′ gd cat-easter. The starting templates were *ea* cDNA (pGEM3) and gdcD7 (DeLotto 2001). The final recombinant PCR fusion was cut with *Bgl*II and *Eco*RI and cloned into pSP64. gdpro and the gdvWF were made by insertion of a stop codon using inverted PCR on the starting plasmids of wild-type full-length gdcD7 and gdΔn_e, respectively. The primers used in the reverse PCR were gd seq7 and gd3′ pro-enz and gd seq7 and 3′ gdvWFe, respectively. The *gd* propolypeptide PCR product was cut with *Not*I and self-ligated, and the gd vWF domain PCR product was cut with *Eco*RI and self-ligated.

mRNA microinjection of transcripts into Drosophila embryos: The mRNA transcripts were synthesized and microinjections performed as previously described (Smith and DeLotto 1994).

RESULTS

Analysis of the phenotypic strength of *gd* alleles: Screens for maternal effect mutations in various laboratories have generated new alleles of *gd* (see materials and methods). We wished to characterize the phenotypic strength of these alleles using the same criteria used in earlier studies (Konrad *et al.* 1988a,b). To distinguish between weak hypomorphic and amorphic alleles, we compared the phenotype of embryos produced by females homozygous for an allele to that of females with the allele over *Df(1)KA10*, a deficiency overlapping *gd*. The phenotypic strength was quantified by scoring embryos into one of four classes. The classes of phenotypic strength employed here were also used in earlier studies of *gd* (Konrad *et al.* 1988b). Class I embryos are strongly dorsalized, lacking both ventral denticles and filzkorper. Class II embryos lack ventral denticles but have filzkorper. Class III embryos are distinguished by the presence of ventral denticles and Class H consists of phenotypically normal embryos, which hatch to larvae. Table 2 shows the results of this analysis for all of the *gd* alleles that we characterized. Overall, our results agree with those previously described for several alleles and the newly isolated alleles fell into the same phenotypic se-

TABLE 2

Determination of the phenotypic strength of alleles of *gastrulation defective*

Allele	No. in each class				Total
	I	II	III	H	
gd^1/gd^1	4	27	69	0	100
$gd^1/Df(1)KA10$	11	89	0	0	100
gd^2/gd^2	100	0	0	0	100
$gd^2/Df(1)KA10$	100	0	0	0	100
gd^3/gd^3	9	7	4	0	20
$gd^3/Df(1)KA10$	44	6	0	0	50
gd^4/gd^4	100	0	0	0	100
$gd^4/Df(1)KA10$	100	0	0	0	100
gd^5/gd^5	0	2	54	44	100
$gd^5/Df(1)KA10$	25	44	31	0	100
gd^6/gd^6	10	90	0	0	100
$gd^6/Df(1)KA10$	56	44	0	0	100
gd^7/gd^7	100	0	0	0	100
$gd^7/Df(1)KA10$	100	0	0	0	100
gd^8/gd^8	100	0	0	0	100
$gd^8/Df(1)KA10$	100	0	0	0	100
gd^9/gd^9	100	0	0	0	100
$gd^9/Df(1)KA10$	100	0	0	0	100
gd^{10}/gd^{10}	100	0	0	0	100
$gd^{10}/Df(1)KA10$	100	0	0	0	100
gd^{190}/gd^{190}	0	5	56	59	100
$gd^{190}/Df(1)KA10$	6	22	69	3	100
gd^{TN124}/gd^{TN124}	22	49	29	0	100
$gd^{TN124}/Df(1)KA10$	91	9	0	0	100
gd^{VM90}/gd^{VM90}	100	0	0	0	100
$gd^{VM90}/Df(1)KA10$	100	0	0	0	100
gd^{VO27}/gd^{VO27}	100	0	0	0	100
$gd^{VO27}/Df(1)KA10$	100	0	0	0	100
gd^{LF12}/gd^{LF12}	100	0	0	0	100
$gd^{LF12}/Df(1)KA10$	100	0	0	0	100
gd^{Li115}/gd^{Li115}	100	0	0	0	100
$gd^{Li115}/Df(1)KA10$	100	0	0	0	100
gd^{LQ4}/gd^{LQ4}	3	4	76	17	100
$gd^{LQ4}/Df(1)KA10$	46	21	32	1	100
gd^{Lu119}/gd^{Lu119}	70	18	12	0	100
$gd^{Lu119}/Df(1)KA10$	57	40	3	0	100
gd^{n27}/gd^{n27}	100	0	0	0	100
$gd^{n27}/Df(1)KA10$	100	0	0	0	100
gd^{p18}/gd^{p18}	1	11	58	30	100
$gd^{p18}/Df(1)KA10$	85	9	6	0	100

ries, varying between amorphic to almost wild type (Konrad *et al.* 1988a,b). We conclude that gd^2, gd^4, gd^7–gd^{10}, gd^{VM90}, gd^{VO27}, gd^{LF12}, gd^{Li115}, and gd^{n27} are amorphic alleles; gd^1, gd^3, gd^6, gd^{TN124}, and gd^{LQ4} are moderate hypomorphic alleles; and gd^5, gd^{190}, gd^{Lu119}, and gd^{p18} are weak hypomorphic alleles.

Interallelic complementation analysis of *gd* alleles: Previous work revealed the existence of three groups of alleles at the *gd* locus (Mohler 1977; Konrad *et al.* 1988a,b). Two groups of alleles exhibited interallelic complementation whereas the third group failed to show any significant interallelic complementation. For the purpose of this analysis, we designated the two groups exhibiting interallelic complementation the gd^2 group and the gd^{10} group, since these two alleles previously exhibited the most dramatic interallelic complementation. The third group, which failed to complement either of the other two groups, we called the noncomplementing group. We performed an interallelic complementation analysis to determine whether the more recently isolated *gd* alleles could also be assigned to these three complementation groups. This was achieved by crossing each allele to gd^2 and gd^1, two members of the gd^2 group, gd^{10} and gd^6, two members of the gd^{10} group, and gd^9, a member of the noncomplementing group. The phenotypic strength of the embryos produced by *trans*-heterozygous females was compared to the sum of the phenotypic strength of the two alleles in a hemizygous state. If the resulting phenotype was significantly shifted toward wild type, the alleles were scored as demonstrating interallelic complementation. The data are presented in Table 3. We found that all of the more recently isolated alleles of *gd* could be classified into either the gd^2 group, the gd^{10} group, or the noncomplementing group. For example, while both $gd^{vo27}/Df(1)KA10$ and $gd^2/Df(1)KA10$ produce only embryos in class I (Table 2), gd^2/gd^{VO27} produces 21/100 embryos in class I, 22/100 embryos in class II, and 57/100 embryos in class III (Table 3). Because it complements gd^2 as well as gd^1, we determined that gd^{VO27} is a member of the gd^{10} complementation group. On the basis of this type of analysis, we concluded that gd^1–gd^3, gd^5, gd^{TN124}, gd^{Lu119}, gd^{LQ4}, gd^{p18}, and gd^{190} are in the gd^2 group, gd^6 and gd^{VO27} are in the gd^{10} group, and gd^4, gd^7, gd^8, gd^9, gd^{Li115}, gd^{LF12}, gd^{n27}, and gd^{VM90} are in the noncomplementing group.

Molecular alterations associated with *gd* mutant alleles: To determine the nature of the changes in mutant alleles of *gd*, both genomic DNA and cDNA were isolated from each of 20 mutant alleles and subcloned. The nucleotide sequence of both the genomic DNA and cDNA was determined and these results are summarized in Table 4. Most alleles revealed deviations from the wild-type nucleic acid sequence that could be correlated with the mutant phenotype. gd^{190}, a weak hypomorphic allele, has a single base change in the second intron, which alters splicing site usage and results in the generation of alternatively spliced transcripts at intron 2 (data not shown). For the alleles gd^1, gd^5, and gd^{p18}, which are hypomorphic or weakly hypomorphic, no nucleotide changes were detected within either the protein coding sequences or within the introns. The positions of the observed changes relative to the protein structure are summarized in Figure 1. Noncomplementing alleles include lesions mapping throughout the protein coding region and, with the exception of gd^7, they contain either a premature stop codon or deletion of part of a coding region. Only gd^7 is predicted to generate a protein with single amino acid substitution. The lesions in the alleles

TABLE 3

Phenotypic strength of *trans*-heterozygous combinations of *gastrulation defective* alleles

Allele	No. in each class				Total	Complementation
	I	II	III	H		
gd^1/gd^{190}	3	18	67	12	100	−
gd^1/gd^{p18}	16	5	20	1	42	−
gd^1/gd^{LQ4}	37	27	36	0	100	−
gd^1/gd^{TN124}	12	19	59	6	96	−
gd^1/gd^{Lu119}	33	29	38	0	100	−
gd^1/gd^{VO27}	0	0	9	91	100	+
gd^1/gd^{Li115}	83	16	1	0	100	−
gd^1/gd^{LF12}	82	18	0	0	100	−
gd^1/gd^{n27}	93	7	0	0	100	−
gd^1/gd^{VM90}	92	7	1	0	100	−
gd^2/gd^{190}	3	31	66	0	100	−
gd^2/gd^{p18}	45	28	27	0	100	−
gd^2/gd^{LQ4}	76	7	17	0	100	−
gd^2/gd^{TN124}	72	24	4	0	100	−
gd^2/gd^{Lu119}	34	18	43	0	95	−
gd^2/gd^{VO27}	21	22	57	0	100	+
gd^2/gd^{Li115}	100	0	0	0	100	−
gd^2/gd^{LF12}	100	0	0	0	100	−
gd^2/gd^{n27}	100	0	0	0	100	−
gd^2/gd^{VM90}	64	0	0	0	64	−
gd^6/gd^{190}	0	0	6	87	93	+
gd^6/gd^{p18}	0	0	11	89	100	+
gd^6/gd^{LQ4}	0	0	15	85	100	+
gd^6/gd^{TN124}	0	0	9	91	100	+
gd^6/gd^{Lu119}	0	0	2	57	59	+
gd^6/gd^{VO27}	95	4	1	0	100	−
gd^6/gd^{Li115}	43	57	0	0	100	−
gd^6/gd^{LF12}	55	45	0	0	100	−
gd^6/gd^{n27}	53	47	0	0	100	−
gd^6/gd^{VM90}	62	38	0	0	100	−
gd^{10}/gd^{190}	0	0	15	85	100	+
gd^{10}/gd^{p18}	0	0	12	88	100	+
gd^{10}/gd^{LQ4}	0	2	41	57	100	+
gd^{10}/gd^{TN124}	0	0	0	10	10	+
gd^{10}/gd^{Lu119}	0	0	4	14	18	+
gd^{10}/gd^{VO27}	100	0	0	0	100	−
gd^{10}/gd^{Li115}	100	0	0	0	100	−
gd^{10}/gd^{LF12}	100	0	0	0	100	−
gd^{10}/gd^{n27}	100	0	0	0	100	−
gd^{10}/gd^{VM90}	100	0	0	0	100	−
gd^9/gd^{190}	3	57	40	0	100	−
gd^9/gd^{p18}	85	13	2	0	100	−
gd^9/gd^{LQ4}	60	13	4	0	77	−
gd^9/gd^{TN124}	83	17	0	0	100	−
gd^9/gd^{Lu119}	56	37	7	0	100	−
gd^9/gd^{VO27}	100	0	0	0	100	−
gd^9/gd^{Li115}	100	0	0	0	100	−
gd^9/gd^{LF12}	100	0	0	0	100	−
gd^9/gd^{n27}	100	0	0	0	100	−
gd^9/gd^{VM90}	100	0	0	0	100	−

gd^{TN124}, gd^2, gd^{Lu119}, gd^3, and gd^{LQ4}, members of the gd^2 complementation group, are clustered within the proenzyme polypeptide after the signal peptide sequence and amino proximal to R_{136} and K_{137}, which in the complement factor C2/B model correspond to the activation cleavage site. All of these lesions result in single

TABLE 4

Alterations identified from nucleotide sequencing of *gd* mutant alleles

Allele	Alteration			Consequence
	DNA	cDNA	Protein	
gd^{1}	—	—	—	
gd^{2}	G86 to A	G86 to A	Cys29 to Tyr	
gd^{3}	C362 to T	C311 to T	Pro104 to Ser	
gd^{4}	G1309 to A	Δ1074-111	915 aa deletion	Splicing error, intron IV acceptor site
gd^{5}	—	—	—	
gd^{6}	T1292 to G	None	None	Within intron IV
	G1714 to A	G1397 to A	Gly466 to Asp	Point near catalytic Ser
gd^{7}	G1768 to A	G1451 to A	Gly484 to Asp	
gd^{8}	C1665 to T	C1348 to T	Gln450 to STOP	Truncates 78 aa
gd^{9}	C1512 to T	C1195 to T	Gln399 to STOP	Truncates 129 aa
gd^{10}	G1723 to A	G1406 to A	Gly469 to Glu	
gd^{190}	G421 to A	—		Alters splicing
gd^{TN124}	C73 to T	C73 to T	Pro25 to Ser	
gd^{VO27}	G1723 to A	G1406 to A	Gly469 to Glu	
gd^{VM90}	(717 bp deletion overlapping 5′ end)			
gd^{LF12}	C892 to T	C697 to T	Gln 233 to STOP	Truncation of 295 aa
gd^{Li115}	—	G1164 to A	Trp388 to STOP	Truncation of 140 aa
gd^{LQ4}	G416 to A	G364 to A	Glu122 to Lys	Splicing altered
gd^{Lu119}	—	C293 to T	Pro98 to Leu	
gd^{n27}	—	A295 to T	Lys99 to STOP	Truncation of 430 aa
gd^{p18}	—	—	—	

aa, amino acid.

amino acid changes within the predicted propolypeptide domain of Gd. The gd^{10} complementation group comprising gd^{6}, gd^{10}, and gd^{VO27} has lesions resulting in single amino acid changes located in close proximity to S_{468}, the predicted active site serine of Gd. The proximity of these lesions to S_{468} suggests that they could affect Gd function by compromising proteolytic activity of the catalytic chain. Thus alterations in gd^{2} group members map to the presumptive proenzyme polypeptide of the C2/B model and those within the gd^{10} group map to the catalytic chain.

Site-directed mutagenesis of gastrulation defective: To test whether amino acid residues critical to serine protease catalysis are required for biological activity of Gd, we altered specific amino acid residues within the coding region of the molecule and used SP6 RNA microinjection to assay for changes in phenotypic rescue. Embryos from gd^{9}/gd^{9} females are completely dorsalized (Table 5). As previously reported, injection of wild-type gdcD7 RNA into embryos from gd^{9}/gd^{9} females locally ventralizes and generates open ventral denticles (DeLotto 2001). We tested whether the presumptive catalytic H_{292} is required by converting it to arginine. As shown, H292R completely eliminated the ability of Gd to restore ventral cuticular features. Alteration of S_{459}, which is located near the presumptive catalytic serine, to alanine

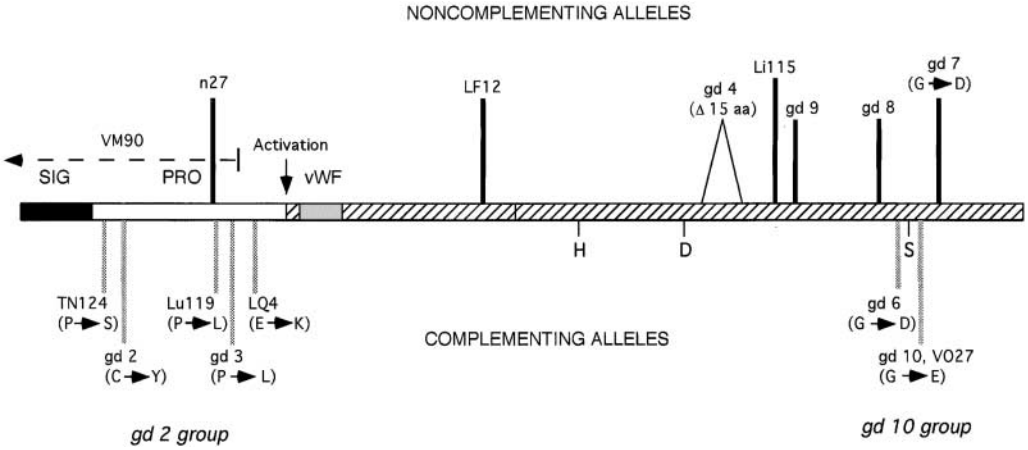

FIGURE 1.—Location of the molecular lesions in GD. Noncomplementing group alleles map throughout the protein coding region. gd^{2} group alleles fall within the presumptive propolypeptide region. gd^{10} group alleles lie close to the active site serine. Both gd^{2} and gd^{10} lesions change amino acids while most of the noncomplementing alleles introduce stops or have deletions.

TABLE 5

Phenotypic rescue assay of site-directed mutants of gastrulation defective into embryos from gd^9/gd^9 females

RNA	No. embryos injected	% cuticles				Gastrulation
		D	FK	VD	HA	
gdcD7 (wt)	125	4	4	96	0	Locally ventralized
$H_{292}R$	108	100	0	0	0	Dorsalized
$S_{459}A$	103	6	5	89	0	Locally ventralized
$S_{468}A$	118	100	0	0	0	Dorsalized
None	200	100	0	0	0	Dorsalized

D, dorsalized; FK, exhibits filzkorper; VD, exhibits ventral denticles; HA, hatching.

had little discernible effect upon the ability of Gd to rescue. However, alteration of S_{468}, the presumptive catalytic serine, to alanine, abolished the restoration of any ventral pattern elements. This last observation is consistent with the mutagenesis of S_{468} leading to loss of a Gd-derived tryptic fragment binding to protease inhibitors and rescue activity (Han *et al.* 2000). We conclude that two of the amino acids involved in the serine protease catalytic triad are critical to biological activity and these results are consistent with Gd functioning biochemically as a serine protease.

Analysis of functional domains proposed by the complement factor C2/B model: If the complement factor C2/B model is correct, a cleavage between R_{136} and K_{137} should produce two polypeptides, an amino-terminally derived propolypeptide and a carboxy-terminally derived catalytic chain. In C2 and B, a domain directly following the cleavage site contains a vonWillebrand factor type A repeat motif, which functions as a binding site for upstream activators. To test the C2/B model, we generated SP6 RNA expressing the full-length Gd protein (wild type), the presumptive catalytic chain (gdΔn_e), the presumptive proenzyme polypeptide (gdpro), or a polypeptide comprising the vonWillebrand factor type A homology (gdvWF). The constructs are illustrated in Figure 2. RNA was microinjected into embryos from various *gd* allelic backgrounds and phenotypic rescue was scored. The results are summarized in Table 6.

Embryos from amorphic gd^9/gd^9, gd^2/gd^2, and gd^{10}/gd^{10} females are completely dorsalized and exhibit no filzkorper (see Figure 3A). When wild-type *gd* RNA is microinjected at >50 μg/ml concentration, the resulting embryos are partially ventralized and exhibit split ventral denticles near the site of injection (Figure 3B). When gdΔn_e RNA was microinjected into embryos from either gd^9/gd^9 or gd^2/gd^2 females, no change in dorsal-ventral cell fate was observed and the embryos remained dorsalized. However, when gdΔn_e RNA was injected into gd^{10}/gd^{10} embryos, 54% of the embryos exhibited either filzkorper or filzkorper and ventral denticles and the gastrulation pattern exhibited polarity. In many embryos the overall cuticular pattern was very close to wild type (see Figure 3C). gd^{10} has a lesion in the presumptive catalytic chain and this result suggests that providing this fragment of Gd as a separate polypeptide can rescue lesions in the catalytic chain.

When gdpro was injected into embryos from either gd^2/gd^2 or gd^{10}/gd^{10} females, no rescue of the dorsalized phenotype was observed. Since we might have expected that gdpro would rescue embryos from gd^2/gd^2 females, we tested for activity of gdpro in wild-type embryos. When gdpro was injected into wild-type embryos, none of the embryos hatched and all of the embryos were partially dorsalized, revealing a dominant negative effect of this polypeptide (see Table 6). This suggests that, while gdpro cannot rescue lesions within the proenzyme polypeptide region, nevertheless, it can affect the patterning system in wild-type embryos. This may occur by binding and competing with some component of the patterning system to downregulate the ventralizing signal. To test whether the activity of full-length Gd could be reconstituted when both the propolypeptide and catalytic chain are provided *in trans*, gdΔn_e and gdpro were microinjected simultaneously into gd^9/gd^9 embryos. In these injections no phenotypic rescue was observed, suggesting that they cannot be supplied as two separate polypeptides to rescue gd^9.

To test the role of the von Willebrand type A motif domain, gdvWF was microinjected into wild-type embryos. No embryos hatched and all of the embryos were to some extent dorsalized, indicating a dominant negative effect of the vonWillebrand factor type A homology domain. To determine how gdvWF alters the Dorsal gradient, we microinjected gdvWF RNA into wild-type embryos and examined the expression of *rhomboid* (*rho*), a marker for the slope and position of the Dorsal gradient, using *in situ* hybridization (Figure 4). In wild-type embryos *rho* is expressed bilaterally as two stripes 6–8 cells wide in a region corresponding to ventral neurogenic ectoderm (Figure 4A; Bier *et al.* 1990). Since it is expressed only in response to intermediate levels of Dorsal, it is a sensitive indicator of the position and slope of the Dorsal gradient (Roth and Schüpbach 1994). When gdvWF RNA is injected into the posterior of a wild-type embryo, the *rho* stripe is widened and shifted ventrally (Figure 4B). This reveals that expres-

TABLE 6

Microinjection of GD domain constructs and autoactivating Snake

RNA	Host	No. embryos injected	% cuticles D	FK	VD	HA	Gastrulation
gdΔn_e	gd^9/gd^9	527	100	0	0	0	Dorsalized
	gd^{10}/gd^{10}	381	46	26	28	0	Polarized
	gd^2/gd^2	358	100	0	0	0	Dorsalized
	+/+	125	35	32	43	0	Partly dorsalized
gdpro	gd^2/gd^2	108	100	0	0	0	Dorsalized
	gd^{10}/gd^{10}	305	100	0	0	0	Dorsalized
	+/+	238	44	29	27	0	Partly dorsalized
gdΔn_e + gdpro	gd^9/gd^9	390	100	0	0	0	Dorsalized
gdvWF	+/+	442	15	29	56	0	Partly dorsalized
XaSnake	gd^2/gd^2	545	100	0	0	0	Dorsalized
	gd^{10}/gd^{10}	285	46	39	15	0	Polarized

D, dorsalized; FK, exhibits filzkorper; VD, exhibits ventral denticles; HA, hatching.

sion of the vWF domain has the effect of dorsalizing and also making the Dorsal gradient shallower. We conclude that the gdvWF domain competes with components of the cascade that are normally required for the regulation of Gd and proper formation of the Dorsal gradient.

Allele-specific interaction with an autoactivating form of Snake: To determine whether Gd directly activates the zymogen form of Snk, we tested for an allele-specific interaction between Gd and Snk. We have previously described a novel form of Snk called XaSnake, which has been mutated in its activation peptide region in such a fashion that the activation peptide sequence resembles its own substrate specificity (Smith *et al.* 1995). The consequence of this mutation is to generate an autoactivating form of Snk. However, microinjection of XaSnake does not result in a dominant ventralizing effect and does not bypass the requirement for upstream functions as was observed with a different construct called snkΔn_e (Smith and DeLotto 1994). Thus XaSnake, while autoactivating, still requires interaction with upstream components to properly exert its function. If Gd is the direct upstream activator of Snk, we reasoned that microinjection of XaSnake into an embryo from a gd^2/gd^2 female would not rescue since a presumptive regulatory function of Gd should be affected in this case. However, XaSnake might rescue embryos from gd^{10}/gd^{10} females since only the activity of the catalytic chain is predicted to be compromised in this case, while the regulatory function of the proenzyme polypeptide should be normal. As expected, when XaSnake RNA was injected into embryos from gd^2/gd^2 females, no phenotypic rescue was observed (Table 6). However, when XaSnake was injected into embryos from gd^{10}/gd^{10} females, 54% of the cuticles exhibited signs of restoration of ventralizing signal and the gastrulation pattern was normally polarized (Figure 3E). This allele-specific interaction between XaSnake and gd^{10} is consistent with biochemical evidence demonstrating GD to be a direct activator of Snk in the protease cascade (Dissing *et al.* 2001; LeMosy *et al.* 2001).

DISCUSSION

The data presented here suggest an explanation for the interallelic complementation observed within the gd^2 and the gd^{10} complementation groups. This interpre-

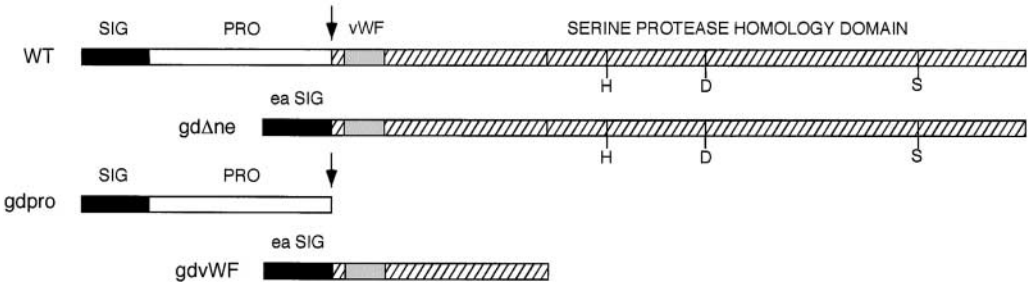

Figure 2.—Diagram of constructs for microinjection. Three deletions relative to the wild-type GD structural gene are illustrated. gdΔn_e fuses the *ea* signal peptide to the presumptive catalytic chain. gdpro truncates at the activation cleavage site. gdvWF begins at the activation cleavage site and terminates at the beginning of homology to serine protease catalytic domains. See materials and methods for details.

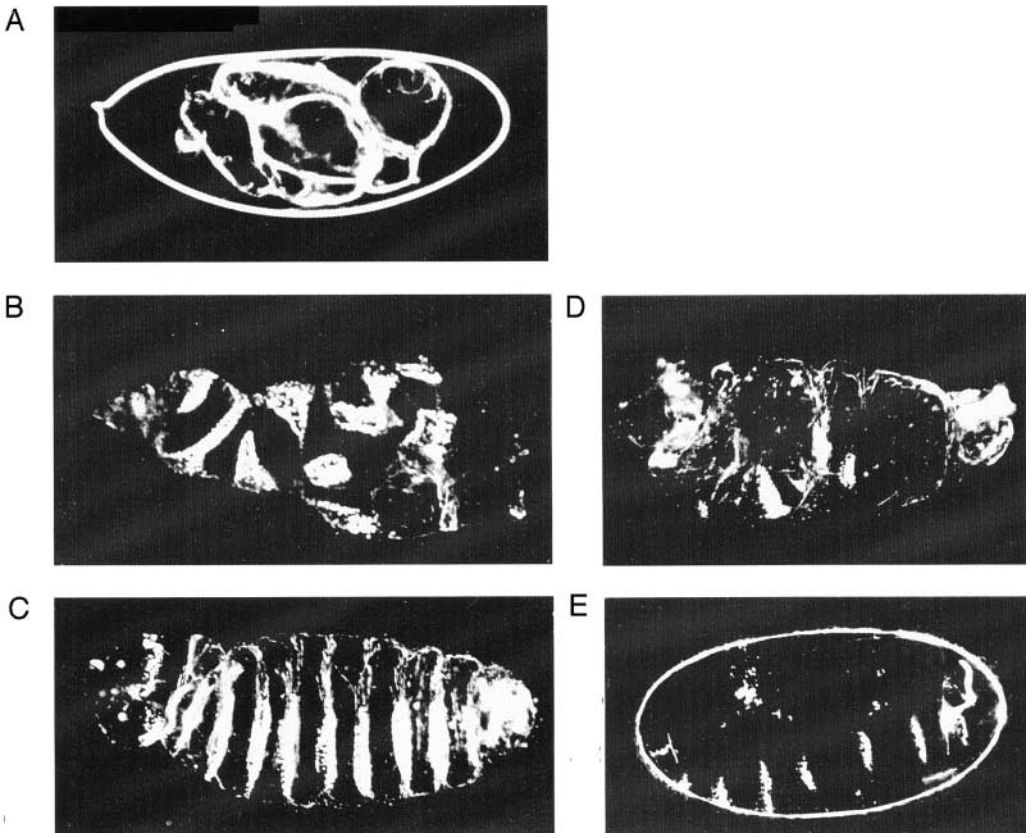

FIGURE 3.—Microinjection phenotypes of embryos. (A) An embryo from a gd^9/gd^9 female. (B) An embryo from a gd^9/gd^9 female injected with wild-type gd SP6 RNA. (C) An embryo from a gd^{10}/gd^{10} female injected with gdΔn_e RNA. (D) An embryo from a gd^{10}/gd^{10} female injected with XaSnk RNA showing restoration of filzkorper, ventral denticles, and head skeleton. (E) An embryo from a gd^{10}/gd^{10} female injected with XaSnk RNA showing uniform width of ventral denticles along the anterior-posterior axis.

tation is also consistent with the complement factor C2/B-like structural model. This C2/B model proposes that Gd, in the process of becoming activated, is cleaved into two separate polypeptide chains. Since all mutations in alleles of the gd^2 group map to the presumptive proenzyme polypeptide, these alterations are expected to specifically alter the activity of the propolypeptide chain. In most serine proteases, this polypeptide is involved in regulating the activity of the catalytic chain by modulating interactions with cofactors and other components of activation complexes in protease activation cascades. The alleles comprising the gd^{10} complementation group have lesions in close proximity to the putative active site serine residue, predicting that they will disrupt the activity of the catalytic chain. Grouping of the alterations to these two regions of Gd would suggest that each part of the Gd protein has an independent biochemical activity.

Whereas interallelic complementation is often due to dimerization or multimerization of a protein, we do not favor this interpretation to explain the interallelic complementation observed at the *gd* locus. First, we have looked for dimerization of Gd using recombinant forms of the protein expressed using the baculovirus system and have found no evidence of either covalent or noncovalent dimers to date (M. DISSING and R. DELOTTO, unpublished results). Second, if proteolytic cleavage at the arginine-lysine pair is part of the normal activation mechanism, then two separate polypeptides would be generated. Complementation would then arise by each allele providing a functional polypeptide consisting of either the catalytic or propolypeptide chain. These two polypeptides appear to have independent biochemical functions and might function sequentially. Alternatively, they may be involved in formation of a larger multiprotein activation complex, something for which there is strong precedent among the coagulation and complement proteases (MANN *et al.* 1988). In this case we might expect that after activation and cleavage two functional polypeptides may associate in an activation complex that can initiate the protease cascade and direct processing of Ea and Spz.

The genetic data indicate that functions mapping to each putative polypeptide chain can in some cases be provided *in trans* to restore normal function to the system. Microinjection of gdΔn_e into embryos from gd^{10} females restores the dorsal-ventral pattern with correct polarity with respect to the asymmetry of the egg. This indicates that the function of the carboxy-terminal catalytic chain may be provided as late as stage 2 of embryonic development. Microinjection of the propolypeptide into embryos from gd^2/gd^2 females did not result in rescue. This may be due to the inability of gdpro to displace a nonfunctional form of the Gd propolypeptide from an activation complex within the PVS. Transplantation experiments with perivitelline fluid revealed activities for Snk, Ea, and Spz, although they failed to find Gd activity (STEIN and NÜSSLEIN-VOLHARD 1992).

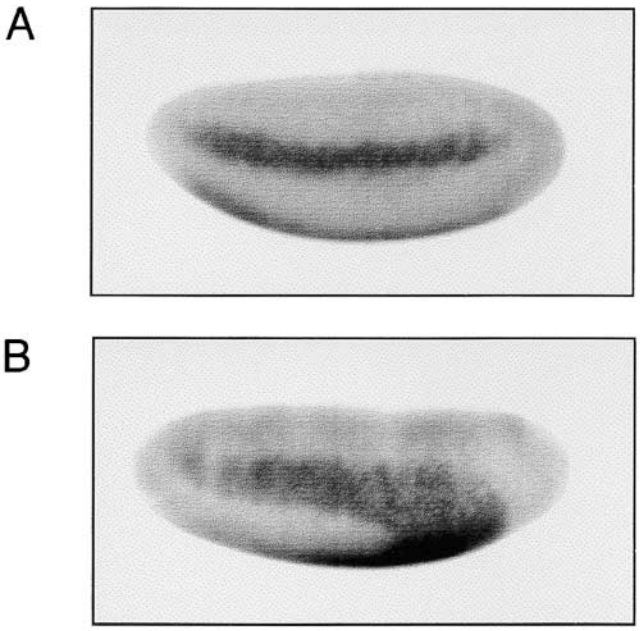

FIGURE 4.—Effect of gdvWF upon wild-type embryos. (A) Rhomboid *in situ* hybridization showing ventrolateral rhomboid stripes in a wild-type embryo. (B) Rhomboid *in situ* hybridization of a wild-type embryo microinjected in the posterior pole with gdvWF RNA showing broadening and ventral displacement of rhomboid stripe. In both A and B, posterior is to the right and ventral is at the bottom.

This result can be interpreted to indicate that Gd is bound to receptors within the PVS at early times during embryonic development. Perhaps gdpro contains binding sites for such a receptor. gdpro can also dorsalize a wild-type embryo when introduced at stage 2. This dominant negative effect indicates that the Gd propolypeptide can interfere with the biochemical pathway in such a way as to reduce the level of the ventralizing signal. However, this competitive effect might be due to interaction with something other than a membrane receptor for Gd and might exert its effect by complexing with and rendering inaccessible the proenzyme of Snk. Similarly, gdvWF, which comprises the vonWillebrand type A homology region, is also able to produce a dominant negative effect when introduced into wild-type embryos. We take these data to indicate that other components of the biochemical pathway interact with this region of the presumptive catalytic chain of Gd. The RNA microinjection result is consistent with the idea that this region might be involved in binding of a positive modulator of activation. However, biochemical aspects of the regulation of Gd are clearly complex and further biochemical analysis of the protein will be necessary.

The allele-specific interaction between gd^{10} and Xa-Snake is consistent with Gd directly activating the Snk zymogen in a protease cascade. When injected into embryos from gd^{9}/gd^{9} females, the catalytic chain of Gd does not rescue or exhibit a dominant lateralizing or ventralizing effect as do analogous constructs for Snk (snkΔN_e) and Ea (eaΔn; CHASAN *et al.* 1992; SMITH and DELOTTO 1994). Therefore, it would appear that both the propolypeptide as well as the catalytic chain are absolutely required for Gd to efficiently activate the downstream components of the pathway.

A role of the propolypeptide in the spatial regulation of Gd activity is supported by the fact that microinjection of gdΔn_e into the posterior pole of an embryo from a gd^{10}/gd^{10} female results in rescue that is uniform along the anterior-posterior axis of the embryo. This contrasts with injection of wild-type *gd* RNA, which produces phenotypic rescue that is greater near the site of injection and less extreme away from the site of injection. The result of injection of gdΔn_e into embryos from gd^{10}/gd^{10} females suggests that the Gd catalytic chain is capable of freely diffusing within the PVS, while full-length Gd is not. This would argue for a localizing or binding function for the Gd propolypeptide.

A model for how Gd functions that fits the ts period data and the genetic and molecular data is as follows. In this model the two separable functions, that of the propolypeptide chain and that of the catalytic chain, are required at two distinct times. Gd protein would be expressed from maternal mRNA late during oogenesis, secreted, and localized to the plasma membrane surface within the PVS via binding sites within the proenzyme polypeptide. Gd is uniformly distributed relative to the dorsal-ventral axis. It remains bound to the plasma membrane and remains inactive until the syncytial blastoderm stage. At this time, Gd becomes autocatalytically active only on the ventral side and initiates a proteolytic cascade resulting in the ventrally restricted production of a processed form of Spaetzle. This "localization during oogenesis/activation during embryogenesis" model explains the ability of Gd to restore ventrolateral pattern elements as late as stage 2 of embryogenesis by microinjection of RNA and its failure to normalize the pattern in embryos from gd^{9}/gd^{9} females. This would be due to the failure to establish the normal distribution of bound Gd within the PVS during embryogenesis because of the nonuniform secretion of Gd into the PVS. Aspects of this model might be tested by generating a heat-shock-inducible form of Gd and a *P*-element-mediated transformed line.

Gd occupies a pivotal role in the process of specifying the dorsal-ventral axis of the embryo. Our data are consistent with Gd directly activating Snk and therefore suggest that Gd is the earliest acting of the germ-line-derived proteases in the PVS. Gd appears to be a molecule intimately involved in the interpretation of the ventral prepattern of the egg (R. DELOTTO, unpublished results). Biochemical data from coexpression experiments indicate that Gd activates Snk and triggers a proteolytic cascade comprising Snk, Ea, and Spz and in the process Gd undergoes rather complex proteolytic processing (DISSING *et al.* 2001). Some of the sizes of these fragments are consistent with predicted sizes for

an active form of Gd from the C2/B model (DeLotto 2001). Taken together, the available data suggest that Gd is responding to spatial prepattern information and to temporal cues for activation and receiving feedback from the cascade that modulates its activity. As Gd is the focus for these multiple inputs, it may constitute a nexus for regulating the shape of the Dorsal gradient. From this perspective, it may not be surprising that complex genetic interactions might be attributed to the *gd* locus.

We thank Boaz Rosenblat for assistance with the DNA sequencing, Marianne Dissing for helpful discussions, Ken Konrad and Anthony Mahowald for providing stocks and information in advance of publication, Trudi Schüpbach for providing stocks, and Gerd Jurgens for helpful discussions. Funding for this work was provided by the U.S. National Science Foundation, the Danish Cancer Fund, the Novo Nordisk Fund, the Vera and Karl Johan Michaelsens Legacy, and the Danish Natural Sciences Research Councils.

LITERATURE CITED

Anderson, K., and C. Nüsslein-Volhard, 1984 Genetic analysis of dorsal-ventral embryonic pattern in *Drosophila*, pp. 269–289 in *Pattern Formation: A Primer in Developmental Biology*, edited by G. Malakinski and P. Bryant. Macmillan, New York.

Anderson, K., and C. Nüsslein-Volhard, 1986 Dorsal group genes of *Drosophila*, pp. 177–194 in *Gametogenesis and the Early Embryo*, edited by J. Gall. A. R. Liss, New York.

Arlaud, G. J., J. E. Volanakis, N. M. Thielens, S. V. Narayana, V. Rossi *et al.*, 1998 The atypical serine proteases of the complement system. Adv. Immunol. **69:** 249–307.

Bier, E., L. Jan and Y.-N. Jan, 1990 *rhomboid*, a gene required for dorsoventral axis establishment and peripheral nervous system development in *Drosophila melanogaster*. Genes Dev. **4:** 190–203.

Chasen, R., and K. V. Anderson, 1989 The role of *easter*, an apparent serine protease, in organizing the dorsal-ventral axis of the *Drosophila* embryo. Cell **56:** 391–400.

Chasan, R., Y. Jin and K. V. Anderson, 1992 Activation of the easter zymogen is regulated by five other genes to define dorsal-ventral polarity in the Drosophila embryo. Development **115:** 607–616.

Clifford, R., and T. Schüpbach, 1992 The torpedo (DER) receptor tyrosine kinase is required at multiple times during Drosophila embryogenesis. Development **115:** 853–872.

DeLotto, R., 2001 Gastrulation defective, a complement factor C2/B-like serine proteose, interprets a ventral prepattern in Drosophila. EMBO Rep. **2:** 721–726.

DeLotto, R., and P. Spierer, 1986 A gene required for the specification of dorsal-ventral pattern in *Drosophila* appears to encode a serine protease. Nature **323:** 688–692.

DeLotto, Y., and R. DeLotto, 1998 Proteolytic processing of the Drosophila Spaetzle protein by Easter generates a dimeric NGF-like molecule with ventralizing activity. Mech. Dev. **72:** 141–148.

DeLotto, Y., C. Smith and R. DeLotto, 2001 Multiple isoforms of the NGF-like growth factor ligand are encoded as alternatively spliced mRNAs in precellular blastoderm embryos. Mol. Gen. Genet. **264:** 643–652.

Dissing, M., H. Giordano and R. DeLotto, 2001 Autoproteolysis and feedback in a protease cascade directing Drosophila dorsal-ventral cell fate. EMBO J. **20:** 2387–2393.

Han, J. H., S. H. Lee, Y. Q. Tan, E. K. LeMosy and C. Hashimoto, 2000 Gastrulation defective is a serine protease involved in activating the receptor toll to polarize the Drosophila embryo. Proc. Natl. Acad. Sci. USA **97:** 9093–9097.

Higuchi, R., 1990 Recombinant PCR, pp. 177–183 in *PCR Protocols: A Guide to Methods and Applications*, edited by M. Innis, D. Gelfand, J. Sninsky and T. White. Academic Press, San Diego.

Konrad, K., T. Goralski and A. Mahowald, 1988a Developmental analysis of *fs(1)gastrulation defective*, a dorsal group gene of *Drosophila melanogaster*. Wilhelm Roux's Arch. Dev. Biol. **197:** 75–91.

Konrad, K., T. Goralski and A. Mahowald, 1988b Developmental genetics of the *gastrulation defective* locus in *Drosophila melanogaster*. Dev. Biol. **127:** 133–142.

Konrad, K. D., T. J. Goralski, A. P. Mahowald and J. L. Marsh, 1998 The gastrulation defective gene of Drosophila melanogaster is a member of the serine protease superfamily. Proc. Natl. Acad. Sci. USA **95:** 6819–6824.

LeMosy, E. K., Y. Q. Tan and C. Hashimoto, 2001 Activation of a protease cascade involved in patterning the Drosophila embryo. Proc. Natl. Acad. Sci. USA **98:** 5055–5060.

Mann, K., R. Jenny and S. Krisnaswamy, 1988 Cofactor proteins in the assembly and expression of blood clotting enzyme complexes. Annu. Rev. Biochem. **57:** 915–956.

Mohler, J.-D., 1977 Developmental genetics of the Drosophila egg. I. Identification of 59 sex-linked cistrons with maternal effects on embryonic development. Genetics **85:** 259–272.

Morisato, D., and K. Anderson, 1994 The *spaetzle* gene encodes a component of the extracellular signalling pathway establishing the dorsal-ventral pattern of the *Drosophila* embryo. Cell **76:** 677–688.

Morisato, D., and K. V. Anderson, 1995 Signaling pathways that establish the dorsal-ventral pattern of the Drosophila embryo. Annu. Rev. Genet. **29:** 371–399.

Neuman-Silberberg, F. S., and T. Schüpbach, 1993 The Drosophila dorsoventral patterning gene gurken produces a dorsally localized RNA and encodes a TGF alpha-like protein. Cell **75:** 165–174.

Oglesby, T. J., M. A. Accavitti and J. E. Volanakis, 1988 Evidence for a C4b binding site on the C2b domain of C2. J. Immunol. **141:** 926–931.

Roth, S., 1994 Proteolytic generation of a morphogen. Curr. Biol. **4:** 755–757.

Roth, S., and T. Schüpbach, 1994 The relationship between ovarian and embryonic dorsoventral patterning in Drosophila. Development **120:** 2245–2257.

Roth, S., D. Stein and C. Nüsslein-Volhard, 1989 A gradient of nuclear localization of the dorsal protein determines dorsoventral pattern in the Drosophila embryo. Cell **59:** 1189–1202.

Roth, S., F. S. Neuman-Silberberg, G. Barcelo and T. Schüpbach, 1995 cornichon and the EGF receptor signaling process are necessary for both anterior-posterior and dorsal-ventral pattern formation in Drosophila. Cell **81:** 967–978.

Rushlow, C., K. Han, J. Manley and M. Levine, 1989 The graded distribution of the *dorsal* morphogen is initiated by selective nuclear transport in *Drosophila*. Cell **59:** 1165–1177.

Schüpbach, T., 1987 Germ line and soma cooperate during oogenesis to establish the dorsoventral pattern of egg shell and embryo in Drosophila melanogaster. Cell **49:** 699–707.

Smith, C., and R. DeLotto, 1994 Ventralizing signal determined by protease activation in *Drosophila* embryogenesis. Nature **368:** 548–551.

Smith, C., H. Giordano, M. Schwartz and R. DeLotto, 1995 Spatial regulation of *Drosophila* Snake protease activity in the generation of dorsal-ventral polarity. Development **121:** 4127–4135.

Stein, D., and C. Nüsslein-Volhard, 1992 Multiple extracellular activities in *Drosophila* egg perivitelline fluid are required for establishment of embryonic dorsal-ventral polarity. Cell **68:** 429–440.

Stein, D., S. Roth, E. Vogelsang and C. Nüsslein-Volhard, 1991 The polarity of the dorsoventral axis in the Drosophila embryo is defined by an extracellular signal. Cell **65:** 725–735.

Steward, R., S. Zusman, L. Huang and P. Schedl, 1988 The *dorsal* protein is distributed in a gradient in early *Drosophila* embryos. Cell **55:** 487–495.

Stroud, R., A. Kossiakoff and J. Chambers, 1977 Mechanisms of zymogen activation. Ann. Rev. Biophys. Bioeng. **6:** 177–193.

Wieschaus, E., and C. Nüsslein-Volhard, 1986 Looking at embryos, pp. 199–228 in *Drosophila: A Practical Approach*, edited by D. B. Roberts. IRL Press, Oxford/Washington, DC.

Communicating editor: A. J. Lopez